

The Application of Hybrid Algorithm Integrating PWM and LMS in Spectrophotometer Instrument Analysis and Anti-Interference Method

Ying Liu*

College of Life and Health, Wuhan Vocational College of Software and Engineering, Wuhan 430205, China

At present, with the rapid development of medical and health undertakings in China, the quality of the results measured by spectrophotometer is improving although the traditional spectrophotometer measurement process is easily disturbed by the stray light noise in the external environment. Therefore, in this study, the LMS (least mean square) adaptive filter is used as the noise filtering device, and PWM (pulse width modulation) is used to collect the original optical signal, and an improved stray light noise filtering algorithm of spectrophotometer is constructed. The test data shows that the average output amplitude of high-level signals after the denoising processing of L-P algorithm, OLS algorithm and LMS algorithm is 1.996. The relative errors of the three algorithms are 0.17%, 1.86% and 0.92% respectively. The L-P algorithm, OLS algorithm, and LMS algorithm denoised the average output amplitude of the low-level signal at 0.000, 0.002, and -0.001, respectively, and the relative errors of the three are 11.41%, 16.95%, and 13.88%, respectively. It shows that the proposed stray light denoising algorithm can extract the stray light in the spectrophotometer to a greater extent than the traditional denoising algorithm, and output a purer useful signal, making it very applicable in fields such as accounting and protein quantification.

Keywords: LMS; PWM; spectrophotometer; stray light noise

1. INTRODUCTION

The spectrophotometer can quantitatively and qualitatively analyze the light absorption properties of the substance being tested. Currently, the spectrophotometer is being used in a number of diverse industries and sectors, particularly those that require precise measurements such as biology, medical care, physics and other disciplines that may involve microbial component identification, tumor detection, outer space exploration, etc. [1, 2]. This is precisely because the

operating accuracy of spectrophotometers in all walks of life is improving day by day. However, the incident light intensity and the transmitted light intensity input by the instrument are easily disrupted by stray light noise, thereby reducing the accuracy of measurement results. Two methods can be used to deal with the stray light interference: hardware suppression and software correction. The former is achieved by grinding and coating some key components of the spectrophotometer to reduce the sensitivity of the instrument to stray light. The purpose of noise reduction, which is more related to the process, is not discussed in this study. When software is used to correct stray light noise, firstly, the optical characteristics

*Email of corresponding author: liuying2130@126.com

of stray light are analyzed, and then modeled and simulated so that most of the stray light noise signal is canceled by the analog signal in the input signal [3]. Currently, the commonly-used stray light denoising algorithms on the market include recursive least squares algorithm, least mean square algorithm, etc., but the denoising effect of these algorithms is still unsatisfactory in some application scenarios with high precision requirements. Therefore, in this study, a stray light denoising method with higher denoising ability is proposed to deal with the spectrophotometer's stray light problem.

2. RELATED WORKS

Previous researchers have carried out extensive academic research on the accurate measurement of spectrophotometer and optical signal denoising, which also has certain reference significance for this research. Some of these research studies are described below. Pozzobon et al. proposed an intelligent algorithm for the design of a spectrophotometric equation to predict the concentration of nitrate and nitrite in experimental samples of algae. The test results showed that the optical signal of microalgae culture samples collected by the spectrophotometer using this algorithm is more accurate [4]. In order to meet the requirements of non-invasive in-vivo spectral analysis, a research team developed a new spectrophotometer to measure the composition changes of main reactants in the redox reaction of plastid cyanin and ferredoxin in vivo. The test results showed that the measurements obtained by this new spectrophotometer were less susceptible to interference from environmental stray light [5]. Matinrad et al. constructed a spectrophotometer with a smart phone application platform. The spectrophotometer integrates simple optical facilities – a tungsten filament lamp as a light source and an electronic multi-functional optical disc – and uses the two as reflection diffraction gratings to study the error source of the smart phone spectrophotometer. An analysis of the optical signal data collected by the spectrophotometer found that the proportional error of heteroscedasticity noise is the most important source of the error and structural change of optical equipment [6]. Dixit compared a mini spectrophotometer with a desktop vis NIR instrument in the spectral range of 900-1700 nm to predict the intramuscular fat (IMF) content of frozen and ground lamb. The prediction results show that the micro spectrophotometer has higher detection accuracy for the intramuscular fat content of the lyophilized and minced lamb meat [7]. Ryan and Mary designed a 3D printable spectrophotometer with dual beam characteristics allowing different types of samples to be collected on the same photo, thereby improving the signal quality and reproducibility of the spectrum [8]. Kuznetsova et al. found that the spectrum of multicolor white visual stimulation partially overlaps the emission spectrum of the indicator, resulting in serious interference with the calcium signal. However, a blue visual stimulation can effectively avoid this problem and improve the detection accuracy of the calcium signal [9]. Clermont's research team found that stray light is the main factor limiting the performance of optical instruments, and accurate simulation of stray light

signals needs to send a sufficient amount of light; however, the simulation of stray light can be very time-consuming. The research team proposed the concept of sending incident stray light into the pupil, and designed a new denoising algorithm based on this idea. The test results show that the denoising operation time of this algorithm is 20% less than that of the traditional algorithm [10]. Hu established a polarization scanning turbidimeter to measure the characteristics of aerosol components in the air, and introduced a new type of a multi hollow-cone optical trap to suppress backscattered stray light. In order to assess the effectiveness of the turbidimeter, a simulation experiment was designed to compare and analyze the denoising effect of the simulation model with and without the optical trap. The experimental results showed that the percentage of backscattered stray light of some particles can exceed 50% without an optical trap. Using an optical trap component comprising several hollow cones, the amount of stray light in the backscattering angle can be reduced to less than 0.7%, and it can be stable at different angles. It shows that this structure is particularly suitable for optical wells with relatively large apertures but insufficient space [11]. In order to mitigate the influence of stray light in the transmission device on the accuracy of the measuring instrument, a polarization isolation single-station system was designed by Yang et al. It uses the polarization isolation principle to isolate stray light. In order to maintain a relatively large scanning angle, the stray light generated by the transmission process is removed. The imaging results of the experiment showed that this method can effectively address the issue of imaging quality of the 1.5 μM laser multi-dimensional vision system that is affected by stray light [12].

To sum up, several technical talents and researchers have carried out studies and experimented with various ideas so as to deal with the influence of stray light on the measurement accuracy of spectrophotometers, aiming to design improved denoising algorithms or adjust and optimize the physical structure of a spectrophotometer. However, these improved methods have limited ability to cope with the time-varying characteristics of stray light, and do not take into account the fact that the distribution characteristics of stray light may vary with the change of wavelength, resulting in a sometimes unsatisfactory denoising effect. Therefore, it is necessary to design a stray light denoising method with better denoising effect and universality.

3. ANTI-STRAY LIGHT NOISE ALGORITHM DESIGN OF SPECTROPHOTOMETER INTEGRATING PWM AND LMS

3.1 LMS Method and Model Design of Adaptive Noise Canceller

In this study, the LMS and PWM methods and the adaptive noise canceller model that constitute the hybrid spectrophotometer anti stray light noise algorithm are designed first,

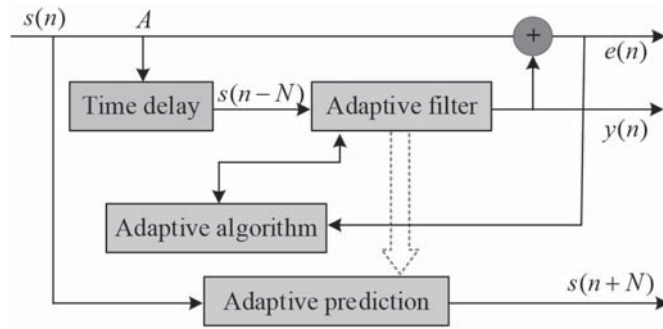


Figure 1 Schematic diagram of a typical structure of an adaptive predictor.

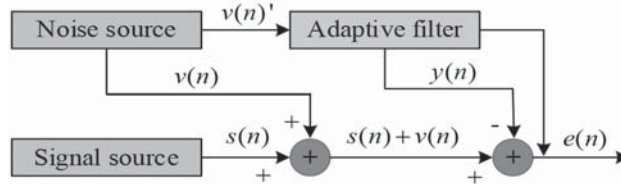


Figure 2 Schematic diagram of the structure of the adaptive noise canceller.

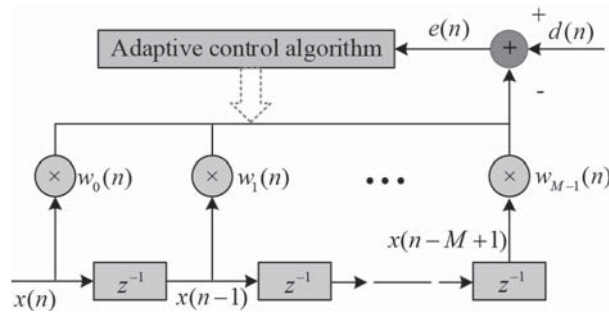


Figure 3 Adaptive Transverse Filter Model.

and then they are combined to create the final stray light noise removal algorithm [13, 14]. The adaptive filter can quickly achieve better filtering effect when the input data parameters are unknown, and has the advantages of simple calculation logic and small calculation amount. Therefore, it is used to process real-time signals [15]. The most important thing is that the adaptive filter can be combined with other adaptive algorithms to further improve the filtering performance. Therefore, the spectrophotometer anti stray light noise algorithm designed in this study will be based on the adaptive filter [16]. The following two common adaptive filters are analyzed to prepare for the subsequent design of LMS adaptive filters.

The adaptive predictor is designed based on the adaptive filter. Its core calculation logic is to appropriately delay the useful signal, and take it as the data to be processed by the filtering device to obtain the best estimation by the adaptive parameter adjustment method, and take it as the fixed parameter of the prediction filter. The system structure of the adaptive predictor is shown in Fig. 1.

Fig. 1 shows the time-delayed signal of the $s(n - N)$ input $s(n)$ signal that can also be understood as $s(n)$ the predicted output of the signal, which is input to the adaptive filter to obtain filtered data $y(n)$, and the residual signal is obtained through comparison and calculation $e(n)$. Usually,

the predictor is structured horizontally. The predictor works by using the useful signal and the adaptive optimal weight coefficient to predict the semaphore of the signal at the next moment. Another common adaptive filter is the adaptive noise canceller; its calculation model is shown in Fig. 2.

Fig. 2 shows that the working principle of the noise canceller: the noise signal and the useful signal are superposed to form a noisy signal, and the signal to be processed is input to the adaptive filter. After the filter parameters are adjusted, the filter outputs the closest estimated value of the noise signal, and then the estimated value of the noise signal is subtracted from the noisy signal in order to cancel the noise interference to a certain extent, so that the residual signal is as close to the useful signal as possible.

The least mean square algorithm (LMS) is an adaptive filtering algorithm with a simple calculation process and wide range of applications. The core of its calculation logic is to use LMS to adjust the weight coefficient of the input signal so that the square between the data to be processed and the filtered signal is as small as possible [17]. This algorithm has the advantages of fast convergence speed, few calculation parameters and simple principle. Therefore, LMS was chosen for the construction of an anti-interference algorithm for a spectrophotometer [18]. The transverse filter structure is shown in Fig. 3.

The transversal filter shown in Fig. 3 above designs an LMS algorithm suitable for spectrophotometer denoising. The weight parameter in the filter $\varpi(n) = [\varpi_1(n), \varpi_2(n), \dots, \varpi_{M-1}(n)]^T$, the input signal vector $x(n) = [\chi(n), \chi(n-1), \dots, \chi(n-M+1)]^T$, the output signal $y(n)$ can be obtained according to Formula (1).

$$y(n) = \varpi^T(n) * x(n) = \sum_{i=0}^{M-1} \varpi_i(n)x(n-i) \quad (1)$$

In Formula (1), n is the sequence length, which M represents the order. The residual signal of the filter can be obtained by Formula (1), and $e(n)$ is calculated with Formula (2).

$$e(n) = d(n) - y(n) = d(n) - \varpi^T(n) * \chi(n) \quad (2)$$

In Formula (2), $d(n)$ is the useful signal corresponding to the signal. $e(n)$ Therefore, according to the minimum mean square error, the filter objective function can be calculated with Formula (3).

$$\varepsilon(n) = [d^2(n)] - 2\varpi^T(n)p + \varpi^T(n)R\varpi(n) \quad (3)$$

In Formula (3), $R = E[x(n)x^T(n)]$, the autocorrelation matrix representing the input signal, the size is $M \times M$, using $P = E[d(n)x(n)]$ the cross-correlation matrix of R representing $d(n)$, and after knowing $x(n)$, and P after, the optimal filtering weight coefficient of the objective function can be obtained by calculating w_0 using Formula (4)

$$w_0 = R^{-1}P \quad (4)$$

According to Formula (4) and Formula (3), the minimum mean square error of the objective function can be obtained. The ε_{\min} calculation formula is shown in Formula (5),

$$\varepsilon_{\min} = E[d^2(n) - w_0^T(n)Rw_0(n)] \quad (5)$$

According to the minimum mean square error, $M \times 1$ the gradient vector of the dimensional signal at time can be obtained, as shown in Formula (6). n

$$\nabla(n) = \frac{\partial E[e^2(n)]}{\partial w(n)} = -E[2e(n)x(n)] \quad (6)$$

According to Formula (6), the updated formula for the filter weight coefficient $w(n+1)$ can be obtained with Formula (7).

$$\varpi(n+1) = \varpi(n) + \mu[-\nabla(n)] \quad (7)$$

where μ represents the adaptive convergence step size, $\nabla(n)$ replace the gradient vector in Formula (7) with the instantaneous estimated gradient vector $\widehat{\nabla}(n)$, and obtain the LMS algorithm representation, see Formula (8).

$$\varpi(n+1) = \varpi(n) + \mu[-\widehat{\nabla}(n)] \quad (8)$$

where $\widehat{\nabla}(n)$ is calculated with Formula (9).

$$\widehat{\nabla}(n) = \frac{\partial E[e^2(n)]}{\partial \varpi(n)} = 2e(n)x(n) \quad (9)$$

According to Formula (9) and Formula (8), the final form of the LMS algorithm iteration formula can be obtained, see Formula (10).

$$\varpi(n+1) = \varpi(n) + 2\mu * x(n) * e(n) \quad (10)$$

Formula (10) μ represents the step size convergence factor. Based on the above derivation content, it can be seen that three main calculation steps of the LMS algorithm are applied to spectrophotometer denoising. First, the parameters required for the algorithm operation are initialized; secondly, the initial condition environment of the algorithm is set and, finally, adaptive signal processing is performed. Input the desired signal and the input signal into the filter for iterative calculation. Next, the performance measurement indicators of the LMS algorithm are designed comprising three indicators: steady-state error, convergence performance and convergence speed. In terms of convergence, the main aim is to make ε_{\min} the expectation of the minimum mean square error converge and obtain the minimum value, and at the same time make the weight coefficient $w(n)$ converge to the mean value; then it needs to satisfy Formula (11).

$$0 < \mu < \frac{1}{(M+1)G} \quad (11)$$

Formula (11) G represents the power of the input signal and M represents the order of the filter. The convergence speed of the algorithm has a high correlation with the convergence time, and the shorter the convergence time, the faster the convergence speed. Formula (12) can be used to define the convergence time of the LMS algorithm.

$$T_{MSE} = \frac{1}{2\mu\lambda_{\min}} > \frac{\lambda_{\max}}{\lambda_{\min}} \quad (12)$$

where λ_{\min} is the minimum value among all the eigenvalues of the autocorrelation matrix in the input signal. The steady-state error of the algorithm is expressed by the offset two, and the offset is P defined according to Formula (13).

$$P = \frac{E[J_e(\infty)]}{J_{\min}} \quad (13)$$

In Formula (13), $J_e(\infty)$ and J_{\min} represent the final value of the minimum mean square error and the estimated value of the minimum mean square error, respectively. In Formula (13), $J_e(\infty)$ is calculated according to Formula (14).

$$J_e(\infty) = E[J_e(\infty)] - J_{\min} = \frac{\mu J_{\min} \sum_{i=1}^M \lambda_i}{2 - \mu \sum_{i=1}^M \lambda_i} \quad (14)$$

λ_i represents the i th eigenvalue, according to Formula (14) and Formula (13), and considering the fact that the μ value is small in practice, Formula (15) is obtained.

$$P = \frac{1}{2}\mu \sum_{i=1}^M \lambda_i \quad (15)$$

There is a linear correlation between the offset P and the algorithm convergence step size. μ , the average eigenvalue can be calculated according to Formula (16) for clarity of understanding

$$\lambda_{av} = \frac{1}{M} \sum_{k=1}^M \lambda_k \quad (16)$$

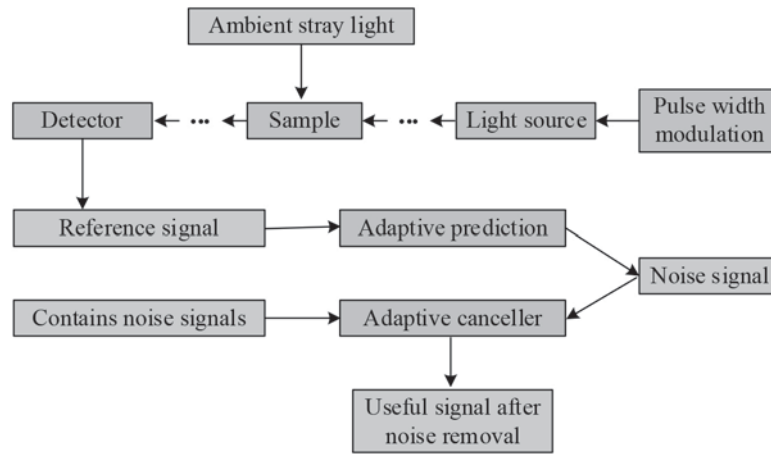


Figure 4 Overall framework design of LP denoising algorithm.

According to this Formula (16) and Formula (15), another formula for calculating the stable offset is obtained, as Formula (17).

$$P = \frac{1}{2} \mu M \lambda_{av} \quad (17)$$

Note that in Formula (17) M represents the order of the filter. It can be seen from Formula (17) that the determinant of the convergence of the algorithm is the step size, the determinant of the convergence speed is the running time of the algorithm and the characteristics of the input signal, and the steady-state error is determined by the filter order and step size convergence parameters. It can be seen that there is a certain inconsistency between the convergence performance, convergence speed and steady-state error of the adaptive filter, and it is impossible to obtain the optimal value of multiple aspects simultaneously. At this point, the LMS algorithm in the anti-interference method of the spectrophotometer has been designed.

3.2 Signal Acquisition Method Based on PWM and Design of Spectrophotometer Anti-Stray Light Method

When collecting signals in real-world scenarios, useful signals and noise signals are often coupled with each other. In order to improve the quality of denoising, the coupling effect of the two should be reduced. Therefore, accurate acquisition of reference signals is a key step in the intelligent denoising process [19]. In the traditional signal processing work, modulation and filtering are used to obtain reference signals. Later, some people have proposed multi-channel reference signal methods to obtain higher-quality signals. However, these methods do not collect the noise and statistical characteristics of the measurement, and can only be used in the measurement. After the data is processed, the accurate acquisition of the spike information in the signal is affected. However, in the current photometric detection, there is generally no equipment for obtaining the reference signal of stray light, which is not good for the accurate extraction of the signal, and a more scientific method is needed to obtain the reference signal of adaptive denoising [20].

Given the characteristics of the reference signal of ambient stray light, this research considers the idea of “time division multiplexing”, and uses the pulse width modulation PWM technology to modulate the light source, thereby converting the original DC optical signal into a periodic intermittent signal. That is f , the PWM pulse signal of the frequency, is used to modulate the light intensity of the light source driven by the constant current power supply to change the light intensity. The principle of the acquisition method of this reference signal is as follows. It is assumed that the noise with a high frequency has a short-term stationary property, or that the stray light T has a short-term stationary property within a period of this frequency condition. Then, a light source is created that can generate a PWM periodic signal. The blocking condition is equivalent to turning off the light source, and the signal collected at this time is regarded as a noise signal. Conversely, the light transmission condition is equivalent to turning on the light source. At this time, the signal of the mobile phone is regarded as a noisy signal. Signal. The signal sampling frequency f_s meets the $f_s \gg f$ condition, the number of samples in one cycle $N = f_s/f$. Therefore, when the PWM is low, because the light source is turned off, there is no diffraction and scattering caused by the light source in the instrument, and the measured data is considered to be $N/2$ the stray light intensity of the length. When the PWM is at a high level, the acquired signal is a noise-containing signal, and the low-level optical signal in the adaptive processing needs to be used as a noise reference signal to provide an accurate denoising reference amount for the noise-containing signal measured in a high-level condition. In addition, light with the same wavelength can be continued for multiple modulation periods to improve noise reduction quality. In the actual measurement, it is necessary to modulate the PWM frequency according to the change in the stray light of the external environment, achieve the on-off adjustment of the light source signal, and ensure the correlation between the obtained reference signal and the noise. Next, the LMS filter and the PWM signal acquisition method is used to construct the spectrophotometer signal anti-interference method (hereinafter referred to as the LP denoising algorithm). The design framework of the LP denoising algorithm is shown in Fig. 4.

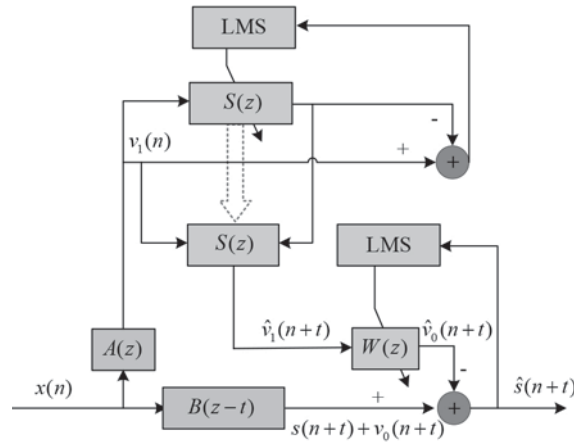


Figure 5 Computational framework of stray light noise point-by-point adaptive correction algorithm.

As shown in Fig. 4, the algorithm comprises three core calculation steps. The first step acquires the input signal. The output signal of the detector should be a periodic signal in the shape of “square wave”. The signal acquired in the low-level state is the reference signal of ambient stray light, and the signal acquired in the high-level state is a noisy signal. The second step predicts the noise signal. Since the noise containing signal and the reference signal are collected at different times, the reference signal cannot be directly used to replace the noise signal in the noise containing signal. However, considering the short-time stationary characteristics of stray light in the period and the one-dimensional and continuity of the reference signal, the reference signal can be used as the filter input to predict the noise in the signal. The last step i cancels the external stray light noise, superimposes the noise prediction signal on the reference end of the adaptive noise canceller, and superimposes the noisy signal at the signal input end. Because the stray light can remain stable in a short period of time, there is a certain correlation between the stray light signal and the noise signal in the noisy signal. Therefore, an adaptive noise canceller is used to cancel the external stray light signal and output a useful signal with higher quality. It can also be seen from Fig. 4 that the principal framework of the point-by-point adaptive correction algorithm is shown in Fig. 5 when testing samples with light sources of the same wavelength.

As shown in Fig. 5, set the PWM half cycle as t , the detector input signal $x(n)$ is processed $A(z)$ and $B(z - t)$ processed to obtain a reference signal $v_1(n)$ and a noise-containing signal $s(n + t) + v_2(n + t)$. $v_1(n)$ After the adjustment, the adaptive filter weight coefficient $S(z)$ is input into the prediction filter to output the predicted noise signal $\hat{v}_1(n + t)$, and then input $\hat{v}_1(n + 1)$ it $s(n + t) + v_2(n + t)$ into the noise canceller, output $\hat{v}_1(n + t)$, compare it with $s(n + t) + v_0(n + t)$, and get $s(n + t)$ the optimal estimated value $\hat{s}(n + t)$. Finally, the overall calculation flow of the stray light LP denoising algorithm of the spectrophotometer is shown in Fig. 6.

As can be seen from Fig. 6, the input signal of the algorithm is the optical signal data collected by the detector. The algorithm captures the stray light reference signal by distinguishing the level state of the input signal, and then uses the LMS filter to achieve fast denoising processing of noisy signals; the output is a useful signal that filters out most of the stray light noise.

4. PERFORMANCE VERIFICATION OF SPECTROPHOTOMETER ANTI-STRAY LIGHT NOISE ALGORITHM

4.1 Design of Simulation Experiment Scheme

In order to test the applicability of the proposed spectrophotometer anti-stray light noise algorithm, a simulation experiment was designed. In the simulation experiment, the useful signal was simulated by a square wave signal, the reference signal representing the ambient stray light signal was simulated by random white noise, and the noisy signal input to the algorithm was formed by the superposition of the previous two signals.

In Fig. 7 is 0.0002, and the useful signal and noise signal are $d(n)$, $v(n)$ respectively $(2\pi t/1000 + \pi)^2 + 1 \cdot (0.1)^{0.5} \times randn(1, N)$. In addition, in order to compare the performance of the LP denoising algorithm, recursive least squares algorithm (ordinary least squares, OLS) and the LMS algorithm were selected for the construction of an alternative denoising algorithm.

4.2 Experimental Results

After the simulation experiment was completed, the processing results of the anti-interference and de-noising algorithms of each spectrophotometer on the noise-containing signal of the simulated signal were sorted out. Firstly, the convergence speed of these algorithms was analyzed from the perspective of the training process of each denoising algorithm. The statistical results are shown in Fig. 8.

In Fig. 8, the horizontal axis represents the number of training iterations of each algorithm, the vertical axis represents the normalized mean square error of each algorithm, and different colors represent different spectrophotometer denoising algorithms. According to the analysis of Fig. 8, the mean square error signal of each algorithm shows a trend of periodic fluctuation and decline in the process of increasing the number of iterations of the algorithm, indicating that the three selected algorithms can remove the stray light noise of

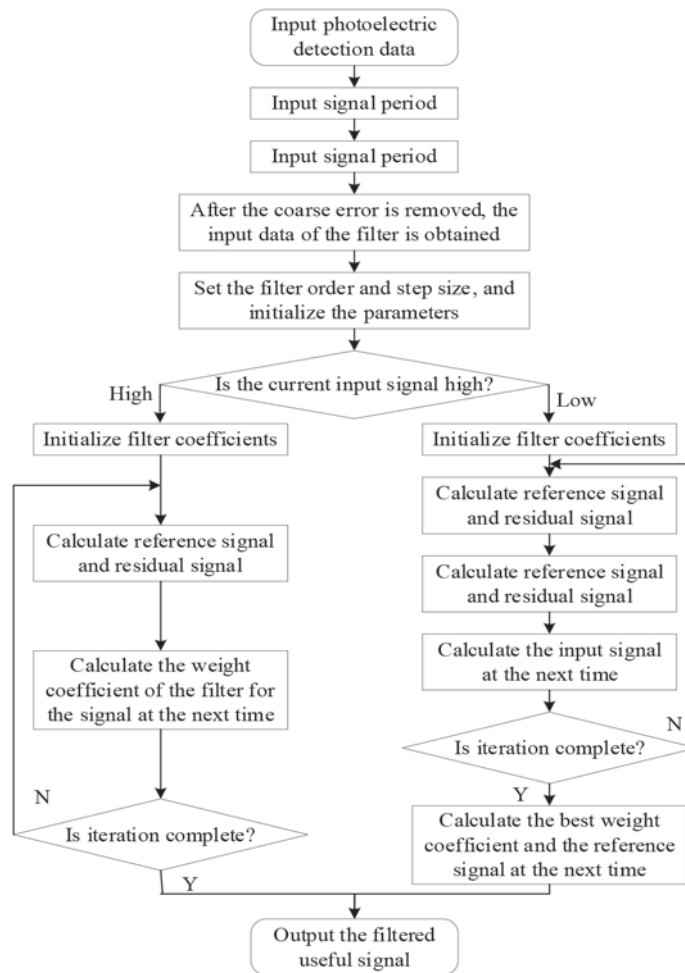


Figure 6 Calculation flow of stray light LP denoising algorithm of spectrophotometer.

the spectrophotometer to a certain extent. But specifically, the OLS algorithm has the fastest convergence speed, but the overall value of the vehicle index is also the highest. The convergence speed of LMS algorithm ranks second, and the mean square error value after convergence also ranks second in the overall level. The L-P algorithm designed in this study has the slowest convergence speed, but the overall mean square error after convergence is also the smallest. From the quantitative point of view, the normalized mean square error values of L-P algorithm, OLS algorithm and LMS algorithm after convergence are about 0.013, 0.018 and 0.043 respectively. Next, the noisy signals processed by the training algorithms are compared. The statistical results are shown in Fig. 9.

In Fig. 9, the horizontal axis represents the duration of the signal in milliseconds, the vertical axis represents the relative amplitude of the output signal of each model, and the lines of different colors represent the waveform diagram of the signal output after the different spectrophotometer stray light denoising algorithms processes the simulated noisy information. Since the output signal has a strong correlation with the period of the noisy signal, only the waveform diagram periods of two complete output signals are used for analysis. It can be seen from Fig. 9 that the three denoising algorithms have poor denoising effect in the low-level state of

the noisy signal, but the denoising effect is significantly better in the high-level state. However, regardless of whether the noisy signal is in the low-level or high-level state, the signal filtering effect of the L-P algorithm proposed in this study is significantly better than the other two methods. From the point of view of quantized data, the average output amplitude of high-level signals after the denoising processing of L-P algorithm, OLS algorithm and LMS algorithm is 1.996, but the relative errors of the three algorithms are 0.17%, 1.86% and 0.92% respectively. The average output amplitudes of low-level signals after denoising by L-P algorithm, OLS algorithm and LMS algorithm are 0.000, 0.002 and -0.001 respectively, and the relative errors of the three algorithms are 11.41%, 16.95% and 13.88% respectively; the denoising effect is stable after 372 ms, 385 ms and 498 ms respectively in each low-level interval. Finally, the residual signals of the noisy signals processed by the training algorithms are analyzed, and shown in Fig. 10.

In Fig. 10, the horizontal axis still represents in milliseconds the duration of the residual signal, and the vertical axis represents the corresponding assignment of the signal. Since the waveform diagram in Fig. 9 proves that the change trend of the output signal of each denoising algorithm in each fluctuation cycle is generally consistent, only the details caused by noise will be different; therefore, here, only one

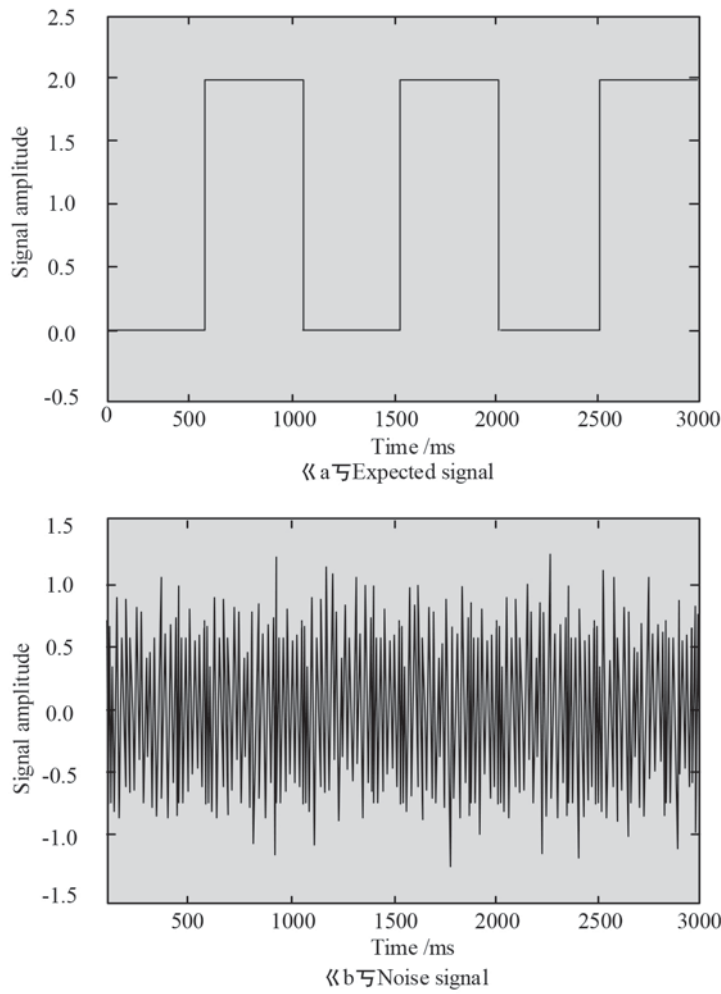


Figure 7 Waveforms of expected signal and noise signal in the simulation experiment.

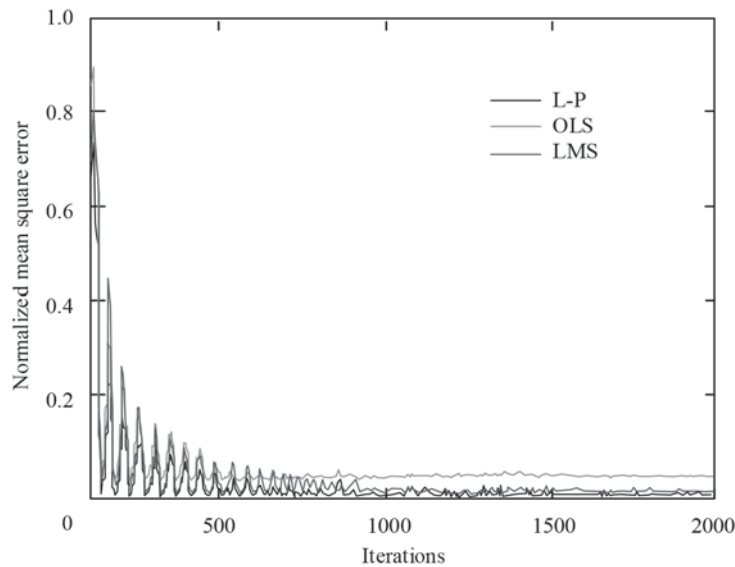


Figure 8 Convergence process comparison of various spectrophotometer stray light denoising algorithms.

complete cycle of the residual signal obtained after processing by each denoising algorithm is selected for analysis. Fig. 10 shows that the residual signal of the output signal processed by the LP algorithm, OLS algorithm, and LMS algorithm

after training generally also has a downward trend in relative amplitude fluctuations with duration in one cycle, and the overall residual of the three. The volatility ranking is consistent with the relative error ranking in Fig. 9, indicating

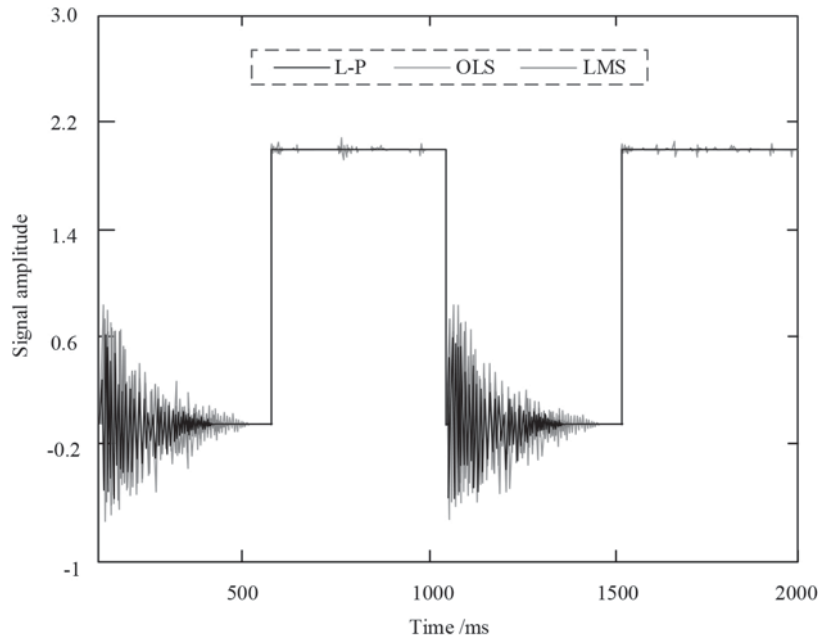


Figure 9 Waveforms of the output signals of the stray light denoising algorithms of each spectrophotometer.

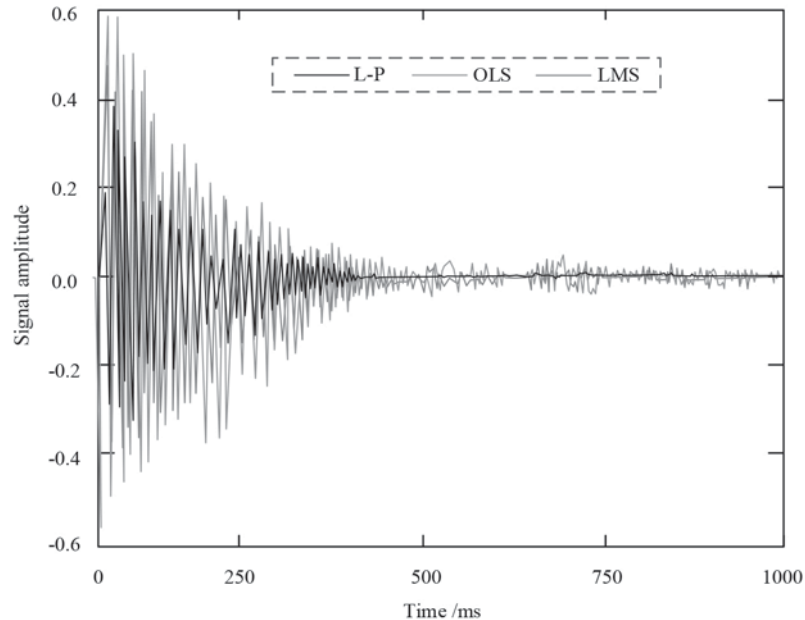


Figure 10 Waveforms of output residual signals of each spectrophotometer stray light denoising algorithm.

that the experimental statistics have strong consistency. Specifically, when the stray light noise denoising residuals of each spectrophotometer tend to converge, the maximum and median residual values of the LP algorithm, OLS algorithm, and LMS algorithm are 0.013, 0.034, 0.051 and 0.004, 0.010, 0.028 respectively.

5. CONCLUSION

In practical applications, the functions of spectrophotometers are easily disrupted by stray light noise, which reduces their effectiveness. Therefore, this research combines LMS and PWM to design a filtering algorithm to filter stray light noise. Simulation experiments were carried out to determine the

performance of the filtering algorithm and compare it with that of another algorithm. The normalized mean square error values after convergence of the L-P algorithm, the OLS algorithm and the LMS algorithm are 0.013, 0.018, and 0.043, respectively. The algorithm designed in this study has the slowest convergence speed during the training phase. The slowest, but the overall mean square error after convergence is also the smallest, while the OLS algorithm has the fastest convergence speed, but the overall mean square error after convergence is also the highest; The average high-level output amplitude of the signal is 1.996, but the relative errors of the three are 0.17%, 1.86%, and 0.92%, respectively. The L-P algorithm, OLS algorithm, and LMS algorithm denoised signal low-level average output amplitudes are 0.000, 0.002, and -0.001 , respectively, and the relative errors of

the three are 11.41%, 16.95%, and 13.88%, respectively. In each low-level interval, the denoising effect of the model is stable through 372ms, 385ms, and 498ms, respectively. The experimental data obtained from simulation show that the stray light denoising performance of the algorithm designed in this study is significantly better than that of the algorithms currently being used in industry. At the same time, due to the limitation of research conditions, no actual data were collected to confirm the superior performance of the algorithm. This will be the focus of future research.

REFERENCES

- Schinke C., Franke M., Bothe K., et al. 2019. Implementation and uncertainty evaluation of spectral stray light correction by Zong's method. *Applied Optics*, 58(36):9998–10009.
- Tol P., Kempen T.V., Hees R.V., et al. 2018. Characterization and correction of stray light in TROPOMI-SWIR. *Atmospheric Measurement Techniques*, 11(7):4493–4507.
- Sandri P., Fineschi S., Romoli M., et al. 2018. Stray-light analyses of the multielement telescope for imaging and spectroscopy coronagraph on Solar Orbiter. *Optical Engineering*, 57(1): 1–18.
- Pozzobon V., Levasseur W., Guerin C., et al. 2021. Nitrate and nitrite as mixed source of nitrogen for *Chlorella vulgaris*: fast nitrogen quantification using spectrophotometer and machine learning. *Journal of Applied Phycology*, 33(3):1389–1397.
- Ginga S., Pierre S., Anja K.L. 2020. Near-infrared in vivo measurements of photosystem I and its luminal electron donors with a recently developed spectrophotometer. *Photosynthesis Research*, 144(1):63–72.
- Matinrad F., Kompany-Zareh M., Omidikia N., et al. 2020. Systematic investigation of the measurement error structure in a smartphone-based spectrophotometer. *Analytica Chimica Acta*, 1129(8):98–107.
- Dixit Y., Pham H.Q., Realini C.E., et al. 2019. Evaluating the performance of a miniaturized NIR spectrophotometer for predicting intramuscular fat in lamb: A comparison with benchtop and hand-held Vis-NIR spectrophotometers. *Meat Science*, 162(Apr):1–9.
- Ryan B., Mary G., A. 2019. 3D-printable dual beam spectrophotometer with multiplatform smartphone adaptor. *Journal of Chemical Education*, 96(7):1527–1531.
- Kuznetsova T., Antos K., Malinina E., et al. 2021. Visual stimulation with blue wavelength light drives V1 effectively eliminating stray light contamination during two-photon calcium imaging. *Journal of Neuroscience Methods*, 362(10):1–29.
- Clermont L., Michel C., Blain P., et al. 2020. Stray light entrance pupil: An efficient tool for stray light characterization. *Optical Engineering*, 59(2):1–9.
- Hu Q., Qiu Z., Hong J., et al. 2019. New light trap design for stray light reduction for a polarized scanning nephelometer. *Review of Scientific Instruments*, 90(3):1–5.
- Yang Q., Jiang Y., He Y., et al. 2018. A method of reducing stray light of 1.5 μ m laser 3D vision system. *Infrared Physics & Technology*, 92(6):266–269.
- Zarubin I.A., Labusov V.A., Babin S.A. 2020. Characteristics of compact spectrometers with diffraction gratings of different types. *Inorganic Materials*, 56(14):1436–1440.
- Yao C., Cheng D., Tong Y., et al. 2018. Design of an optical see-through light-field near-eye display using a discrete lenslet array. *Optics Express*, 26(14):18292–18299.
- Chng J., Patuwo M.Y. 2021. Building a raspberry pi spectrophotometer for undergraduate chemistry classes. *Journal of Chemical Education*, 98(2):682–688.
- Huang C., Zhang M., Chang Y., et al. 2019. Directional polarimetric camera stray light analysis and correction. *Applied Optics*, 58(26):7042–7049.
- Zou Z.Y., Liu H.Q., Ding W.X., et al. 2018. Effects of stray lights on Faraday rotation measurement for polarimeter-interferometer system on EAST. *Review of Scientific Instruments*, 89(1):013510–013518.
- Zhang C., Guo C., Zhang D. 2018. Ship navigation via GPS/IMU/LOG integration using adaptive fission particle filter. *Ocean Engineering*, 156(15):435–445.
- Xue X., Ying L., Qiang S. 2018. Unmanned aerial vehicle object tracking by correlation filter with adaptive appearance model. *Sensors*, 18(9):2751–2766.
- Abadi M., Shafiee M.S., Zalaghi M. 2018. A low computational complexity normalized subband adaptive filter algorithm employing signed regressor of input signal. *Eurasip Journal on Advances in Signal Processing*, 2018(1):21–32.